 doi:10.20944/preprints201810.0506.v1

Discussion on the Peak Shift of A-Ti Phase in Tio_2 Nanostructured Coatings on Ti-6Al-4V Alloy

Linh Nguyen Thi Truc [a,*], Zhong-Tao Jiang[c], Jaegyu Kim[b], Seungbum Hong[b], Kwangsoo No[b]

[a] Department of Chemistry, Ho Chi Minh City University of Pedagogy, Ho Chi Minh City, Viet Nam
[b] Korea Advanced Institute of Science and Technology, Department of Materials Science and Engineering, Daejeon, South Korea
[c] Surface Analysis and Materials Engineering Research Group, School of Engineering and Information Technology, Murdoch University, Murdoch, WA 6150, Australia

[*]Corresponding author:
Dr. **Linh Nguyen Thi Truc,** Department of Chemistry, Ho Chi Minh City University of Pedagogy, 280 An Duong Vuong, Ward 4, District 5, Ho Chi Minh City (Postal code: 700000), Viet Nam, linhntt@hcmup.edu.vn

Abstract

In this study, TiO_2 nanostructured coatings on Ti-6A-4V alloys were fabricated by two methods: H_2O_2 oxidation and RF sputtering. In the annealing temperature range of 25 °C - 500 °C, there were the peaks at 35°, 37°, 40° and 52° corresponding to {100}, {002}, {101} and {102} crystal planes of hcp structure of α-Ti. At the annealing temperature of 600 °C, there was the presence of peaks corresponding to crystal planes of anatase and rutile TiO_2. The relative intensities of anatase and rutile phases of the sample fabricated by RF sputtering were 3.62 and 10.25 %, respectively; while those of the sample fabricated by H_2O_2 oxidation were 21.27 and 3.20 %, respectively (The relative intensity of α-Ti phase was 100 %). The results investigated the peak shift of α-Ti phase in TiO_2/Ti-6Al-4V nanostructured coatings fabricated by the two methods which was reasonably explained from the difference in the thermal expansion coefficients of Ti alloy and TiO_2 components, as well as the difference in the ratio of anatase to rutile phases.

Keywords: *Nanostructures; Crystallites; Physical vapor deposition processes; TiO_2; Ti6Al4V alloy*

Introduction

Ti-6A-4V ELI (Extra Low Interstitial) alloy (Grade 5, ASTM) has been widely used as a biomedical material in the medical industry due to its biocompatible (adj) and mechanical (adj) characteristics (noun) such as its good machinability, superior tensile, specific strength, fracture toughness, low weight ratio and corrosion resistance within the human body [1,2]. To achieve

Preprints (www.preprints.org) | NOT PEER-REVIEWED | Posted: 22 October 2018 doi:10.20944/preprints201810.0506.v1

biocompatibility, osteoconductivity, and osseointegration, it is necessary to modify the surface of Ti-6Al-4V alloy by developing hydroxyapatite (HAp, $Ca_{10}(PO_4)_6(OH)_2$) coating on its surface [3-9]. HAp composite materials, which is a bonding interface to stimulate bone apatite and collagen production, improves bone anchorage due to osseointegration for long periods [10]. J. Dumbleton *et al*. [11] have proven that HAp coating should be in crystalline form which has an ability to provide a better substrate for the development of cells, to prevent the formation of adverse fibrous tissue. To increase the adhesion strength of HAp coating on the substrate, it should exhibit sub-layers between HAp coating and Ti-6Al-4V surface [12]. The addition of the sub-layers is expected to reduce a thermal expansion mismatch of the layers, as well as to achieve an abundance of surface hydroxyl and superoxide radicals groups, consequently, to achieve a surface free of cracks and a high adhesion of the modified surface to the substrate [13,14]. Kim H. W. *et al*. [15] investigated that the insertion of a TiO_2 buffer layer was to improve the bonding strength between the HAp layer and Ti substrate, as well as to prevent the corrosion of the Ti substrate. The results reported in the publication [15] showed that the bonding strength of the HAp/TiO_2 double layer coating on Ti markedly increased, with the highest strength of the double layer coating at 55 MPa after annealing at 500 °C. Annealing the coating at the high temperature to keep the surface of hydroxyapatite stable, which is important for the interaction between hydroxyapatite substrate and bone tissue cells. Moreover, annealing the coating is to obtain nanostructured coatings with pre-determined structure, chemical and phase composition [16]. Other publications have also discussed the proper temperature to improve the strength and quality of the titanium–hydroxyapatite interface in the annealing temperature range of 500 – 750 °C [17-20]. However, at the high annealing temperature, the values of thermal expansion coefficients of Ti alloy and TiO_2, as well as those of HAp and TiO_2 should be concerned carefully. In this research, at the beginning, we focused on the difference in thermal expansion coefficients of Ti alloy and TiO_2 components. According to the literature [21], the SI units of the coefficient of thermal expansion is K^{-1} and typical values for alloys are in the range of 10×10^{-6} to 30×10^{-6} K^{-1}, and this value of Ti alloy is 8.70×10^{-6}/K. The computed linear thermal expansion coefficient (TEC) of TiO_2, which is similar with the experimental data, is 6.55×10^{-6} K^{-1} [22]. Some original results determined the effect of the difference in the TEC values, as well as the preparation methods on the structure of TiO_2 sub-layer on Ti-6A-4V alloy. The main aim of study is to investigate the peak shift of α-Ti phase in TiO_2/Ti-6Al-4V

Preprints (www.preprints.org) | NOT PEER-REVIEWED | Posted: 22 October 2018 doi:10.20944/preprints201810.0506.v1

nanostructured coatings fabricated by a controlled oxidation in hydrogen peroxide *via* RF magnetron sputtering technique.

Material and methods

The specimen used for this study was Ti–6Al–4V alloy (Gr 5, ASSTM 136, BAOJI TI-LEADER METAL PROCESSING CO., LTD) with a circular shape of 10.0 mm diameter and 1.0 mm thickness. The specimens were polished using the abrasive silicon carbide (SiC) paper up to 1200 grade. Final polishing was done using 0.02 – 0.25 µm corundum grits (Struers AP-Paste SQ) and micro-cloth (40-72222, Buehler, Vibromet 2) to obtain a surface without scratch, followed by rinsing with distilled water and acetone in ultrasonic.

Preparation of TiO_2 coating on Ti-6A-4V alloy *via* RF magnetron sputtering method: Using a TiO_2 target (High Purity Chemicals Lab. Corp., Grade: 99.99%) as the source material and Ar gas (99.99%) as the sputtering gas. An RF generator was used at a frequency of 13.56 MHz and a power of 100 W. Ar gas was then introduced into the vacuum chamber by a mass flow controller at 50 sccm and kept at 5.0×10^{-3} mbar as the total pressure. Before the deposition of the samples, the chamber was kept in the pre-sputtering regime for 10 min (shutter closed) to remove contaminations on the target surface in order to stabilize the deposition parameters. Ti-6Al-4V surfaces were fixed onto the substrate holder which was centrally positioned in parallel just above the source material with a target- to-substrate distance of 60 mm. The deposition time was 2 hours.

Converting Ti-6Al-4V surface to TiO_2/Ti-6Al-4V by the controlled oxidation in hydrogen peroxide: Ti-6Al-4V after polishing were subjected to oxidation in 30 % solution of H_2O_2 (Purity Chemicals Lab, Korea) at 70 °C for 48 hours.

The TiO_2 nanostructured coatings on Ti-6A-4V alloy were annealed in a vacuum furnace at 25 Torr and the rate of temperature increase of 10 °C /min, kept at the highest temperature (400, 500 and 600 °C) for 2 hours and cooled freely down to the room temperature.

The structure and phase composition of the surfaces were investigated *via* X-ray powder diffraction (XRD, Rigaku Ultima JV, Japan) with Cu Kα radiation (λ = 1.540 Å), the acquisition time of 4° per minute, and the step size of 0.01.

Preprints (www.preprints.org) | NOT PEER-REVIEWED | Posted: 22 October 2018 doi:10.20944/preprints201810.0506.v1

Results and discussion

Fig. 1 displays that in the annealing temperature range of 25 °C to 500 °C, there were only four diffraction peaks at 35°, 37°, 40° and 52° (symbolized as ■) corresponding to {100}, {002}, {101} and {102} crystal planes of hexagonal close packed (hcp) structure of α-Ti, respectively (JCPDS database 44-1294). At the annealing temperature of 600 °C, it can be observed the presence of two extra peaks at 25.2° and 47.9° (symbolized as ▲) corresponding to {101} and {200} crystal planes of tetragonal structure of TiO_2 anatase phase (JCPDS database 84-1286). In addition, the peaks of TiO_2 rutile phase appeared at 27.4° and 54.4° (symbolized as Δ) corresponding to {110} and {211} crystal planes (JCPDS database 88-1175).

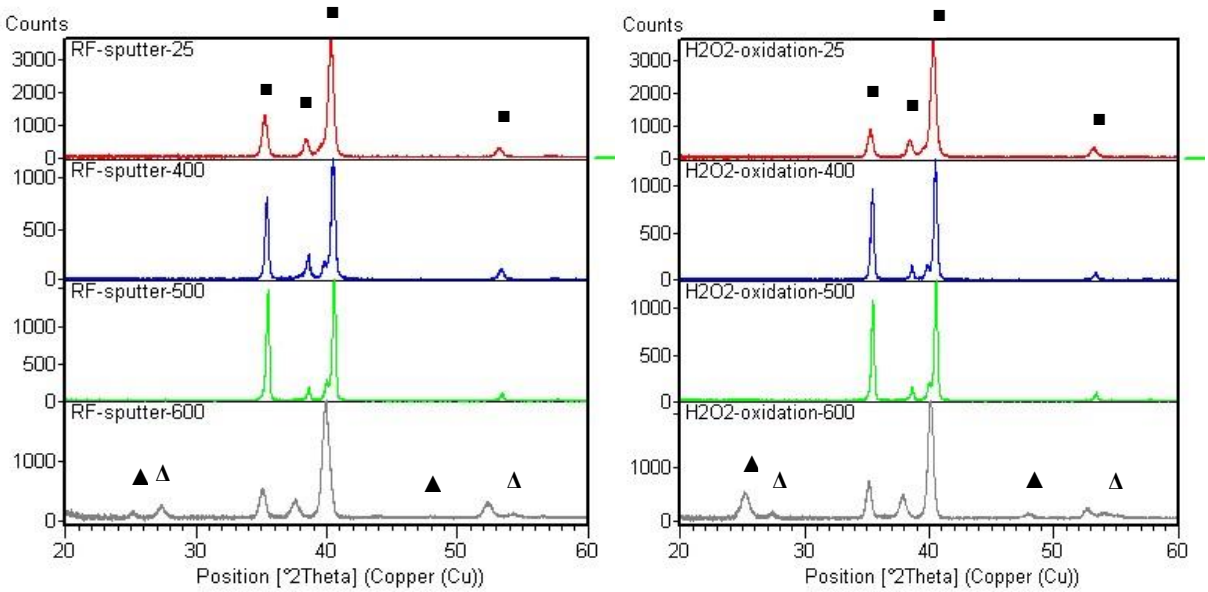

(a) RF sputtering (b) H_2O_2 oxidation

Fig. 1: XRD patterns of TiO_2/Ti-6A-4V samples annealed in the range of 25 °C to 600 °C

Remarkably, the peak shift phenomenon of all four diffraction peaks of α-Ti phase was observed in XRD pattern of TiO_2/Ti-6A-4V alloy annealed at 600 °C, while these peaks did not shift in all the cases of TiO_2/Ti-6A-4V alloy annealed in the range of 25 °C to 500 °C, as well as those of Ti-6A-4V alloy annealed at 600 °C. The central positions of these peaks shifted to lower 2-theta side, consequently, the corresponding *d* spacing values of the reflections increased (Table 1). Changes in lattice spacing of titanium crystalline were presented in some publication as following: R. Montanaria *et al.* [28] investigated the effects of nitrogen and oxygen absorption

Preprints (www.preprints.org) | NOT PEER-REVIEWED | Posted: 22 October 2018 doi:10.20944/preprints201810.0506.v1

on lattice expansion of Ti–6Al–4V by high-temperature X-ray diffraction. After annealing this material at 600 °C, the oxygen or nitrogen atoms may occupy in the octahedral interstices of (hcp) structure of α-Ti, which results in the expansion of cell volume and the changes in the ratio of cell parameters. According to the literatures [29, 30] mechanical and physical properties of titanium alloys strongly depend on interstitial elements at high temperature. The nature of the reinforcement/matrix interface plays a significant role in the stress transfer of the composites, thus influences the mechanical properties of composites.

Table 1: *d* spacing values of the reflections {100}, {002}, {101} and {102} of α-Ti existing in TiO_2/Ti-6A-4V samples annealed at various temperatures

{hlk}	**d spacing (nm)**					
	25 °C	**400** °C	**500** °C	**600** °C		
				Ti alloy	**H_2O_2 oxidation**	**RF sputtering**
{100}	25.44	25.42	25.41	25.44	25.50	25.61
{002}	23.34	23.38	23.37	23.45	23.70	23.87
{101}	22.31	22.30	22.28	22.32	22.45	22.57
{102}	17.16	17.12	17.14	17.17	17.36	17.46

In this study, oxygen and nitrogen elements may not exist in the coatings due to annealing in a vacuum furnace. Thus, the TiO_2 film, which was crystallized in anatase and rutile phases, formed onto the surface of Ti-6A-4V alloy and affected on the structure of the original alloy as the temperature increased up to 600 °C. In fact, the thermal expansion coefficient (TEC) of Ti alloy was 8.70×10^{-6}/K and that of TiO_2 was 6.55×10^{-6} K^{-1}. The TEC, which is one of the structural parameters, was given as a reason in the increase of d spacing values of the reflections of TiO_2/Ti-6A-4V alloy annealed at the phase transition temperature of TiO_2. The TEC of Ti alloy is larger than that of TiO_2, so the rate of contraction of TiO_2 layer should be smaller than that of Ti substrate during cooling, which resulted in the lattice expansion.

Particularly, Table 1 also presents that the degree of lattice expansion of the sample fabricated by the controlled oxidation in hydrogen peroxide was less than that of the sample synthesized by the RF magnetron sputtering method. This result can be explained by the difference in the thermal expansion coefficients of anatase and rutile phases, as well as the difference in the ratio of the two phases in the samples fabricated by the different processes. To determine the relative ratios of anatase phase to rutile phase coexisting in TiO_2/Ti6Al4V

Preprints (www.preprints.org) | NOT PEER-REVIEWED | Posted: 22 October 2018 doi:10.20944/preprints201810.0506.v1

samples, the strongest reflections for anatase and rutile phases were conveniently located at 25.2° and 27.4°, after baseline correction (Fig. 2).

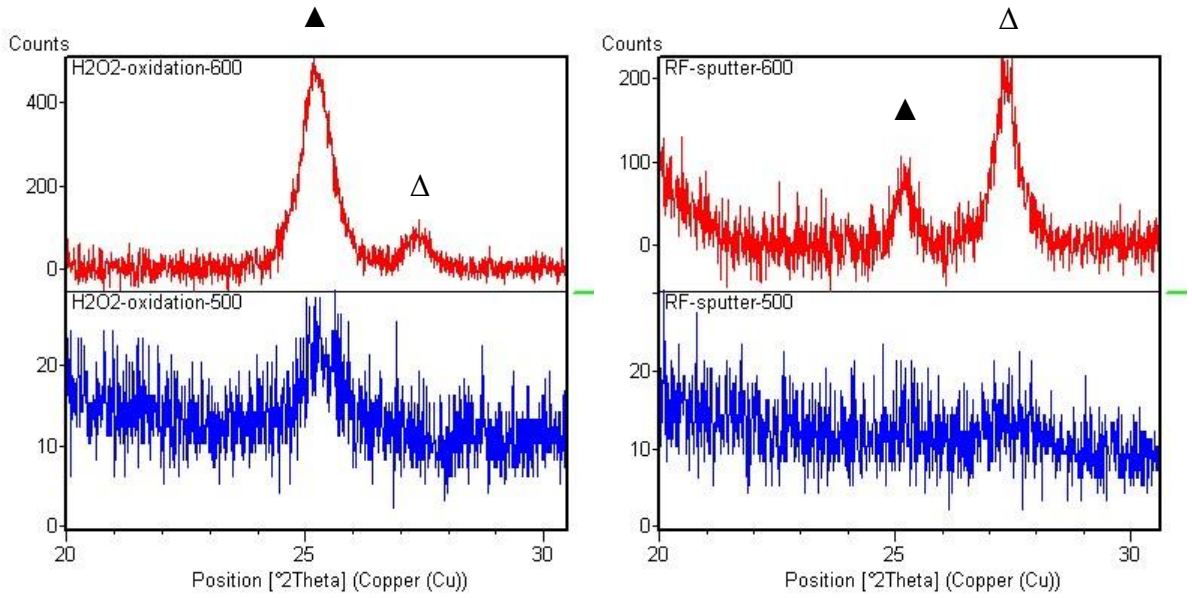

(a) H_2O_2 oxidation (b) RF sputtering

Fig. 2: The presence of the peaks in the 2-theta range of 20-30° of the samples annealed at 500 °C and 600 °C, where anatase phase is symbolized as ▲, and rutile phase is symbolized as Δ

Fig. 2 investigated the difference in the temperature of formation of anatase, rutile phases in the two fabrications, as well as in the ratio of anatase phase to rutile phase. Firstly, the anatase phase appeared in the sample fabricated by the H_2O_2 oxidation after annealing at 500 °C, while this phase did not appear in the sample fabricated by RF sputtering at the same annealing temperature. Moreover, the sample fabricated by RF sputtering had an amount of rutile phase increasing fast after annealing from 500 to 600 °C. According to James's explanation (J. Ovenstone *et al.* [27]), the presence of a small amount of brookite phase contamination in the anatase resulted in rapid conversion to the rutile. In case of the sample fabricated by the controlled oxidation in hydrogen peroxide, the amount of anatase phase was higher than that of rutile phase, while the sample fabricated by the RF magnetron sputtering method had an opposite ratio. This result means TiO_2 coatings sputtered *via* RF sputtering may contain a small amount of brookite phase, however, that was not confirmed by XRD examination. Secondly, the difference in the ratio of anatase phase to rutile phase was identified due to the relative intensity (%) of the peaks (Table 2).

Preprints (www.preprints.org) | NOT PEER-REVIEWED | Posted: 22 October 2018 doi:10.20944/preprints201810.0506.v1

Table 2: Data of the peaks at 25.2° and 27.4° of the samples annealed at 500 °C and 600 °C

Sample	Phase	Position [°2Th.]	FWHM [°2Th.]	Relative Intensity [%]	Crystallite size (nm)
RF-sputter-600	Anatase	25.22	0.472	3.62	16.2
	Rutile	27.38	0.551	10.25	13.8
	α-Ti	39.92	0.708	100	-
Oxidation-600	Anatase	25.18	0.629	21.27	12.2
	Rutile	27.42	0.629	3.20	12.1
	α-Ti	40.15	0.472	100	-

Table 2 also showed the crystallite sizes of the anatase and rutiles phases coexisting in TiO_2/Ti6Al4V samples. In case of the sample fabricated by the oxidation, the widths of peaks at 25.2° and 27.4° for anatase and rutile phases, respectively, were practically the same, so anatase and rutile crystallites had the same size. While the sample fabricated by RF sputtering had the sizes of anatase and rutile crystallites were slightly higher. The difference in crystallite sizes calculated from XRD data was appropriate to that in particle sizes observed from SEM images (Fig. 3). Thus, the degree of lattice expansion of α-Ti phase in the sample fabricated by the H_2O_2 oxidation was less than that in the sample fabricated by the RF sputtering because of two reasons: First, the TEC of TiO_2 anatase was smaller than that of TiO_2 rutile in the same condition [31]. Second, the amount of anatase phase was higher than that of rutile phase in the case of the sample fabricated *via* H_2O_2 oxidation process.

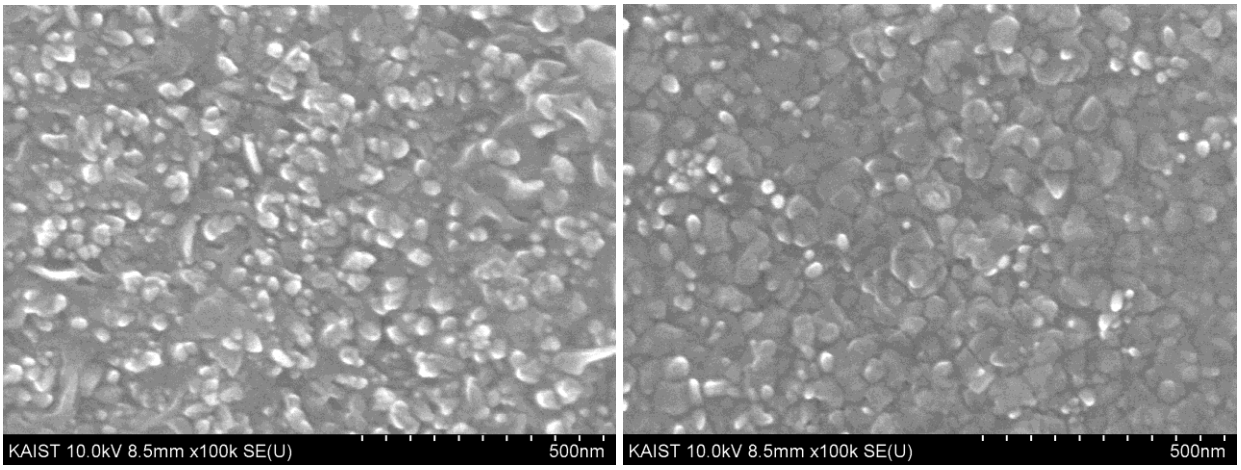

(a) H_2O_2 oxidation (b) RF sputtering

Fig. 3: SEM images of the samples annealed at 600 °C

Conclusion

 doi:10.20944/preprints201810.0506.v1

In summary, we successfully synthesized TiO_2 nanostructured coatings on Ti-6A-4V alloy by both H_2O_2 oxidation and RF sputtering. The results investigated the peak shift of the reflections {100}, {002}, {101}, and {102} of α-Ti existing in TiO_2/Ti-6A-4V materials at the high annealing temperature. The relative intensities of anatase and rutile phases of the sample fabricated by RF sputtering were 3.62 and 10.25 %, respectively; while those of the sample fabricated by H_2O_2 oxidation were 21.27 and 3.20 %, respectively (The relative intensity of α-Ti phase was 100 %). It is deduced that the difference in the thermal expansion coefficients of Ti alloy and TiO_2 components, as well as the difference in the ratio of anatase to rutile phases were the main reason of changes in lattice spacing of α-Ti phase.

Author Contributions

Linh Nguyen Thi Truc, Jaegyu Kim conducted the experiments and prepared the figures and tables. Kwangsoo No, Seungbum Hong contributed to data analysis and interpretation. Linh Nguyen Thi Truc and Zhong-Tao Jiang wrote the main manuscript text. All authors including Linh Nguyen Thi Truc, Jaegyu Kim, Zhong-Tao Jiang, Seungbum Hong, Kwangsoo No reviewed the manuscript.

Additional Information

Competing interests All authors declare no competing interests.

Acknowledgement

This research was supported by Small Grant Scheme (2017) of the SEIT, Murdoch University and by Basic Science Research Programs (No. 2015R1D1A1A01056983) through the NRF, Korea, funded by the Ministry of Education, and (No. 2018R1A2B6002194) through the NRF, Korea funded by the Ministry of Science and ICT.

References

[1] Morais L. S., Serra G. G., Muller C. A., Andrade L. R., Palermo E. F., Elias C. N., Meyers M., Titanium Alloy Mini-Implants for Orthodontic Anchorage: Immediate Loading and Metal Ion Release, Acta Biomaterialia, 3 (3) (2007), pp. 331–339

[2] C. N. Elias, J. H. C. Lima, R. Valiev, M. A. Meyers, Biomedical applications of titanium and its alloys, Volume 60, Issue 3, pp 46–49 (2008)

[3] Sandrini E, Giordano C, Busini V, Signorelli E, Cigada A., Apatite formation and cellular response of a novel bioactive titanium, J. Mater. Sci. Mater. Med. 18 (2007) 1225–1237

[4] Peng Yu, Fang Lu, Wenjun Zhu, Di Wang, Xiaojing Zhu, Guoxin Tan, Xiaolan Wang, Yu Zhang, Lihua Li, Chengyun Ning, Bio-inspired citrate functionalized apatite coating on rapid prototyped titanium scaffold, Appl. Surf. Sci. 313 (2014) 947–953

[5] C. Aparicio, D. Rodriguez, F. J. Gil, Variation of roughness and adhesion strength of deposited apatite layers on titanium dental implants, Mater. Sci. Eng. C 31 (2011) 320–324

[6] Dianying Chen, Eric H. Jordan, Maurice Gell, Mei Wei, Apatite formation on alkaline-treated dense TiO_2 coatings deposited using the solution precursor plasma spray process, Acta Biomater. 4 (2008) 553–559

[7] Hae-Won Kim, Young-Hag Koh, Long-Hao Li, Sook Lee, Hyoun-Ee Kim, Hydroxyapatite coating on titanium substrate with titania buffer layer processed by sol–gel method, Biomaterials 25 (2004) 2533–2538

[8] A. Balamurugan, G. Balossier, J. Michel, J. M. F. Ferreira, Electrochemical and structural evaluation of functionally graded bioglass-apatite composites electrophoretically deposited onto Ti6Al4V alloy, Electrochim. Acta 54 (2009) 1192–1198

[9] M.Chellappa, U.Vijayalakshmi, Electrophoretic deposition of silica and its composite coatings on Ti-6Al-4V, and its in vitro corrosion behaviour for biomedical applications, Materials Science and Engineering C xxx (2016) xxx–xxx, in press

[10] Ravi Krishna Brundavanam, Zhong-Tao Jiang, Peter Chapman, Xuan-Thi Le, Nicholas Mondinos, Derek Fawcett, Gérrard Eddy Jai Poinern, Effect of dilute gelatine on the ultrasonic thermally assisted synthesis of nano hydroxyapatite, Ultrasonics Sonochemistry 18 (2011) 697–703.

[11] Dumbleton J, Manley MT., Hydroxyapatite-coated prostheses in total hip and knee arthroplasty. Journal of Bone and Joint Surgery - Series A. 2004; 86(11): 2526-40

[12] V. M. Ievlev, E. P. Domashevskaya, V. I. Putlyaev, Yu. D. Tret'yakov, S. M. Barinov, E. K. Belonogov, A. V. Kostyuchenko, M. I. Petrzhik, F. V. Kiryukhantsev-Korneev, Structure, elemental composition, and mechanical properties of films prepared by radio-frequency magnetron sputtering of hydroxyapatite. Glass Physics and Chemistry. 2008; 34(5):608-16

[13] Takemoto S, Yamamoto T, Tsuru K, Hayakawa S, Osaka A, Takashima S., Platelet adhesion on titanium oxide gels: effect of surface oxidation, Biomaterials 25 (2004) 3485–3492

[14] P Tengvall B Wälivaara J Westerling I Lundström, Stable titanium superoxide radicals in aqueous Ti-peroxy gels and Ti-peroxide solutions, J. Colloid Interface Sci. 143 (1991) 589–592

[15] Kim HW, Koh YH, Li LH, Lee S, Kim HE, Hydroxyapatite coating on titanium substrate with titania buffer layer processed by sol-gel method, Biomaterials. 2004 Jun; 25(13):2533-8

[16] K. Van Dijk, H. G. Schaeken, J. C. G. Wolke, C. H. M. Maree, F. H. P. M. Habraken, J. Verhoeven, and J. A. Jansen, Influence of discharge power level on the properties of hydroxyapatite films deposited on Ti6A14V with RF magnetron sputtering, Journal of Biomedical Materials Research, Vol. 29, 269-276 (1995)

[17] A. Carradò, F. Perrin-Schmitt, Q.V. Le, M. Giraudel, C. Fischer, G. Koenig, L. Jacomine, L. Behr, A. Chalom, L. Fiette, A. Morlete, G. Pourroy, Nanoporous hydroxyapatite/sodium titanate bilayer on titanium implants for improved osteointegration, Dental Materials (2016)

[18] Mohammadi S, Esposito M, Hall J, Emanuelsson L, Krozer A, Thomsen P. Short-term bone response to titanium implants coated with thin radiofrequent magnetron-sputtered hydroxyapatite in rabbits. Clin Implant Dent Relat Res 2003; 5: 241–253

[19] Zhi xin Kang, Junyi Zhang, Lei Niu, A one-step hydrothermal process to fabricate superhydrophobic hydroxyapatite coatings and determination of their properties, Surface and Coatings Technology, Volume 334, 25 January 2018, Pages 84-89

[20] Rad AT, Novin M, Solati-Hashjin M, Vali H, Faghihi S., The effect of crystallographic orientation of titanium substrate on the structure and bioperformance of hydroxyapatite coatings, Colloids Surf B Biointerfaces 2013;103:200–8

[21] J D James, J A Spittle, S G R Brown and R W Evans, A review of measurement techniques for the thermal expansion coefficient of metals and alloys at elevated temperatures, Measurement Science and Technology 12 (2001) R1–R15

[22] S.L.Tang, Y.R.Wang, Y.M.Gao, Q.L.Zheng, D.W.Yi, Theoretical study of mechanical and thermodynamic properties of titanium oxides Ti_xO_y, Materials Chemistry and Physics, 2018, In Press, Accepted Manuscript

[23] M. Karthega, N. Rajendran, Hydrogen peroxide treatment on Ti–6Al–4V alloy: A promising surface modification technique for orthopaedic application, Applied Surface Science, Volume 256, Issue 7, 15 January 2010, Pages 2176-2183

[24] Nishiguchi S, Nakamura T, Kobayashi M, Kim HM, Miyaji F, Kokubo T., The effect of heat treatment on bone-bonding ability of alkali-treated titanium. Biomaterials 1999; 20:491-500

[25] C.Guillén, J.Herrero, TiO_2 coatings obtained by reactive sputtering at room temperature: Physical properties as a function of the sputtering pressure and film thickness, Thin Solid Films, Volume 636, 31 August 2017, Pages 193-199

[26] Jaspal Singh, Saif A.Khan, J.Shah , R. K. Kotnala, Satyabrata Mohapatra, Nanostructured TiO_2 thin films prepared by RF magnetron sputtering for photocatalytic applications, Applied Surface Science, Volume 422, 15 November 2017, Pages 953-961

[27] James Ovenstone, and Kazumichi Yanagisawa, Effect of Hydrothermal Treatment of Amorphous Titania on the Phase Change from Anatase to Rutile during Calcination, C*hem. Mater.*, 1999, *11* (10), pp 2770–2774

[28] R. Montanaria, G. Costanza, M.E. Tata, C. Testanib, Lattice expansion of Ti–6Al–4V by nitrogen and oxygen absorption, Materials characterization 59 (2008) 334 – 337

[29] Simbi DJ, Schully JC. The effect of residual interstitial elements and iron on mechanical properties of commercially pure titanium. Mater Lett 1996; 26:35–9

[30] Ouchi C, Iizumi H, Mitao S. Effects of ultra-high purification and addition of interstitial elements on properties of pure titanium and titanium alloys. Mater Sci Eng A 1998; 243: 186–95

[31] K. V. Krishna Rao, S. V. Nagender Naidu, Leela Iyengar, Thermal Expansion of Rutile and Anatase, Journal of the American Ceramic Socisty, Volume 53, Issue 3, 1970, 124-126